Proton Transfer on the Edge of the Salt/Co-Crystal Continuum: X-ray Photoelectron Spectroscopy (XPS) of Three Isonicotinamide Salts

Paul T. Edwards,[1] Lucy K. Saunders,[2] Anuradha R. Pallipurath,[1] Andrew J. Britton,[1]

*Elizabeth A. Willneff,[3] Elizabeth J. Shotton,[2] Sven L. M. Schroeder[1,2]**

[1]School of Chemical and Process Engineering, University of Leeds, Leeds, LS2 9JT, UK
[2]Diamond Light Source Ltd, Harwell Science and Innovation Campus, Didcot, Oxfordshire OX11 0DE, UK
[3]School of Design, University of Leeds, Leeds, LS2 9JT, UK
[4]Future Continuous Manufacturing and Advanced Crystallisation Hub, Research Complex at Harwell (RCaH), Rutherford Appleton Laboratory, Harwell, Didcot, Oxon, OX11 0FA, UK

* Sven L. M. Schroeder:

Email: s.l.m.schroeder@leeds.ac.uk

Abstract

X-ray photoelectron spectroscopy (XPS) has emerged as a technique that allows for characterisation and classification of hydrogen bonding and proton transfer interactions in organic crystal structures, in a way that is complementary to crystallography by X-ray or neutron diffraction. Here we analyse the nitrogen 1s core level binding energies of isonicotinamide systems with proton transfer between donor and acceptor groups at short distances. We show how a careful calibration of the binding energy scale places these salt systems correctly on the edge of the so-called salt-co-crystal continuum. We show how performing a fitting analysis of the data that is consistent with elemental analysis, expected stoichiometry, and quantification of adventitious carbon contamination facilitates the determination of absolute binding energies with accuracy and reproducibility within ±0.1 eV. The determined N 1s core level binding energies of the protonated isonicotinamide acceptors suggests that the local geometric arrangements of donor, acceptor and proton can influence the N 1s core level binding energy significantly.

Introduction

Creating crystals with an organic co-former is a widely used approach for tailoring the physical properties of pharmaceuticals and other functional organic compounds.[1] In the presence of proton donor-acceptor pairs, electrostatic interactions often drive the supramolecular assembly process, so the difference in pK_a values of donor and acceptor groups is often used for physical property prediction.[2,3] For ΔpK_a differences > 3, proton transfer, and hence the formation of ionic salts is observed.[4–13] For negative ΔpK_a values, hydrogen bonding occurs and the product is classified as a co-crystal.[4–13] Between these two regimes, in the ΔpK_a range of 0…3, the nature of the donor-acceptor interaction is generally unpredictable and other properties, for example other non-covalent interactions, conformational variations and steric factors, can tip the balance from proton transfer to hydrogen bonding and vice versa. This region is often referred to as the salt co-crystal continuum.[7,11,14,15] It comprises not only examples of structures with proton-transfer or hydrogen-bonding, but also many cases that elude such classification, especially when donor-acceptor bond distances are short.[10] As a result, structures with proton transfer and short donor-acceptor distances have variously been referred to as salts,[4,5,13] charge-assisted short strong hydrogen bonds[16,17] or proton transferred interactions.[8,10,12,14,18] Co-crystals are usually described as hydrogen-bonded or containing neutral hydrogen bonds,[4,5,13,19] but short donor-acceptor distances can, for example, result in short-strong hydrogen bonds (SSHBs) in which the proton is partially transferred, but shared between donor and acceptor,[10] blurring the boundary between salt and co-crystal. Moreover, systems with multiple options for donor-acceptor pairing often exhibit two or more types of interactions within one crystal structure – the systems to be examined in this paper includes an example of such cases.[16]

Various studies[8–12] have demonstrated that the core level binding energy shifts detected at the acceptor by X-ray photoelectron spectroscopy (XPS) are sensitive to the position of the proton. Studies of a substantial range of salts and co-crystals with nitrogen acceptors have shown that the N 1s core level binding energy consistently discriminates Brønsted proton transfer (salts) from hydrogen bonding (co-crystal) through a chemical shift of approximately 2 eV.[7,10,11,14,15] Whether hydrogen bonding or proton transfer take place is determined by the relative depths of the double-well potentials associated with the Brønsted interaction,[10] while the proton position is determined by the location of the potential minimum relative to donor and acceptor. The core level binding energy shifts, in donor-acceptor systems, reflect the local charge density variation induced by the proton. XPS thus highlights the electrostatic force exerted by the proton, at both the donor and the acceptor centres. Simply put, the negative charge at the donor site increases as the proton is more distant, while the positive charge at

the acceptor increases as the proton comes closer. In this view, one has a continuum of electrostatic field effects on donor and acceptor, which is influenced by the distance between donor and acceptor centres as well as their individual distance to the proton. Systems in which the donor-acceptor distance is short (up to ~2.6 Å) allow strong potential well overlap, resulting in a low barrier or even a single well without any barrier.[10] Often referred to as short hydrogen bonds (SHBs) or short strong hydrogen bonds (SSHBs), their classification into salt and co-crystal is not clear-cut when the barrier is so low that the protons are able to populate a continuum of positions, and with a distribution that responds to temperature variations.[7,10,16,20] In line with this, XPS distinguished a quasi-centered population of hydrogens in a low-barrier SHB between an oxygen donor and a nitrogen acceptor unequivocally.[10] Compared to the N 1s emission from protonated and hydrogen-bonded functional groups, broadening of the N 1s emission line reflected the dynamic disorder in the quasi-single potential well, and the N 1s emission line centroid was at an intermediate binding energy (BE), neither characteristic for protonation nor for a hydrogen bond.[10]

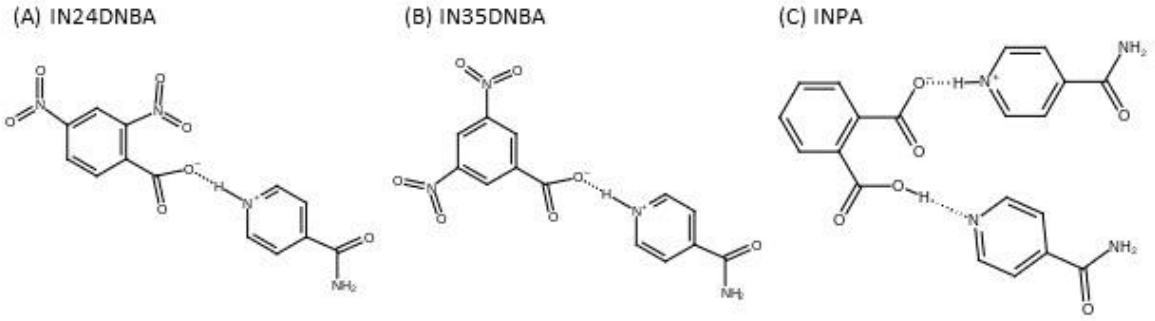

Figure 1. Chemical structures investigated comprising three two component isonicotinamide-acid (base-acid) systems with (a) 2,4-dinitrobenzoic acid (1:1), (b) 3,5-dinitrobenzoic acid (1:1) and (c) phthalic acid (2:1). N-H-O distances can be found in the supplementary material Table S1.

Recently, multi-component molecular crystals containing short strong hydrogen bonds (SSHBs) have been engineered by combining substituted organic acids with isonicotinamide (IN).[16] In the isonicotinamide 2,4-dinitrobenzoic acid (IN24DNBA) and isonicotinamide 3,5-dinitrobenzoic acid (IN35DNBA) 1:1 complexes (Figure 1) an interaction takes place between the carboxylic acid group OH donor and the pyridinic N acceptor of IN. In the case of isonicotinamide phthalic acid (INPA, Figure 1), the 2:1 IN:PA ratio of the components means two distinct interactions are present, between each of the carboxylic acid OH groups of phthalic acid (PA) and a pyridinic N of the two IN co-

formers.[16] All three complexes are within the salt co-crystal continuum, i.e. in the range $0 < \Delta pK_a < 3$. Using X-ray crystallography, the hydrogen atom positions were determined using Fourier difference maps of the electron density.[16] It was found that IN formed charge-assisted hydrogen bonds with both 2,4- and 3,5-dinitrobenzoic acid, characterised by Brønsted proton transfer from the carboxylic acid to the pyridinic nitrogen group.[15,16] This suggests the existence of a sloping potential well, with its minimum located near the nitrogen acceptor. Phthalic acid in INPA had distinct intermolecular interactions with each of its two IN co-formers. One carboxylic acid group formed an SHB characterised by Brønsted protonation (as in IN24DNBA and IN35DNBA), while the other formed a more conventional hydrogen bond with the proton located nearer to the donor.[16] Our interest in applying XPS to these systems stems from their complementarity to our previous study of a quasi-centred SHB.[10] As in that study, O-N donor-acceptor distances in all three complexes are within the range of an SHB,[21] but in contrast to the quasi-centred SHB we have studied previously,[10,16] the Fourier difference maps indicated that the proton is located at the nitrogen acceptors as a result of proton transfer.[10,16] One of the reasons for examining these complexes further by XPS is that the relative proximity of the electrostatic potential from the donor may influence the charge at the acceptor sufficiently to result in a detectable N 1s core level shift relative to a non-SHB salt. If so, then XPS would distinguish protonation in a charge-assisted SHBs from conventional Brønsted proton transfer with a longer donor-acceptor distance, allowing a more nuanced classification of salts.

The expected effect on the N 1s BE was expected to be smaller than the BE shift associated with protonation, requiring a highly accurate determination of BE shifts. In addition to examining the mentioned effect on the N 1s core level binding energy, we therefore provide a detailed description of our data analysis procedure, to enable other researchers to follow this protocol and facilitate wider use of XPS for the characterisation of Brønsted interactions in organic crystals. The key to success of such studies is a reliable calibration of the core level electron BE scale with accuracy and precision (reproducibility) within ±0.1 eV for all investigated samples.[22] Throughout our work over the last decade we have found that such accuracy can be achieved by careful calibration of the BE scale through self-consistent analysis of the elemental composition and quantitative analysis of the C 1s emission line.[7–12,14,23] This facilitates accurate identification of the energy position of the aliphatic carbon contribution from adventitious carbon contamination present on the samples. This procedure overcomes the inaccuracies associated with the use of less elaborate BE scale calibrations based on C 1s emission from adventitious carbon.[24–26] We will demonstrate how the use of adventitious carbon as an internal BE standard can provide a very consistent calibration when a complete fitting analysis of

the C 1s emission line is performed. We have reliably applied this procedure throughout all of our previous studies of organic systems, as it removes the uncertainties associated with taking the overall maximum of the C 1s emission line as the BE calibration peak. Using this method, the absolute N 1s binding energy involved in H-bonding is consistently found to be in the range 399 eV - 400 eV, while a salt is found between 401 eV - 402 eV.[7–12,14,23]

Experimental Methods

Materials

All three samples were prepared by evaporation from solution, as described in previous work.[16] The crystallizations were carried out in methanol (INPA) and ethanol (IN24DNBA and IN35DNBA) using a 2:1 stoichiometric ratio (INPA) or 1:1 ratio (IN24DNBA and IN35DNBA). Prior to measurement, crystalline samples were crushed to form a powder. In addition, pure isonicotinamide (IN, 99.9%) for XPS analysis was obtained from Flurochem.

X-ray Photoelectron Spectroscopy (XPS)

XP spectra were collected with a SPECS EnviroESCA NAP-XPS equipped with a monochromatic Al K-alpha X-ray source (1486.71 eV) operating at 42 W separated from the analysis chamber with a SiN window which illuminated the sample with a ~300 µm diameter beam footprint. Spectra were collected on powder samples pressed onto double sided adhesive carbon tape at ambient temperature in 7 mbar argon with a hemispherical Phoibus NAP 150 analyser operating in small-area mode with a source-analyser angle of 55° and a 1D delay-line detector. Under NAP conditions in the EnviroESCA instrument, insulating sample surfaces are inherently charge-neutralized through ionization of the gas phase by the X-ray beam, which provides positive ions and electrons to balance any surface charge.[26,27] Survey spectra were collected in one scan with a step size of 1 eV, pass energy of 100 eV and dwell time of 0.1 s. High resolution C 1s, N 1s, and O 1s core level spectra were collected with a step size of 0.1 eV, a dwell time of 100 ms per data point, and a pass energy of 50 eV. Spectra for C 1s and O 1s core levels were collected in 9 scans. Due to the lower atomic abundance of N within the sample, the N 1s core level spectrum was collected in 16 scans. The spectra were analysed using CasaXPS.[28] Shirley backgrounds were used and a GL(30) line shape (30% Lorentzian, 70% Gaussian) to fit the emission lines with appropriate components to describe the environment of each element in the sample.[29]

Quantitative Elemental Analysis

From early on in our XPS studies of organic materials we have found that quantitative elemental analysis of a wide-scan survey spectrum provides crucial boundary conditions for the correct interpretation of the C 1s emission line (Figure S1).[30] Identification of non-functionalised hydrocarbon contributions ('adventitious carbon') to the C 1s emission line is the most widely used binding energy calibration method for organic compounds (*vide infra*). Initially, the survey spectra were checked to ensure the number and BEs of the emission lines were broadly consistent with the stoichiometry of the materials. Then it was ensured that the correct spectrometer transmission function was applied.[31,32] The transmission function is specific to the spectrometer and is influenced by various experimental parameters, such as the angles between X-ray source, sample and analyser entrance, operational detector and transfer lens settings, gas phase composition and pressure (for NAP instruments).[28,31,32] It must be re-determined when any changes to these settings are made. Having successfully carried out these intensity calibrations, the elemental composition analysis is performed in CasaXPS[28] to determine the detected atomic percentage of each element within the probed sample volume.[29] Comparison with the expected stoichiometry of the sample then allows the determination of the excess carbon quantity, C_{adv}, resulting from adventitious contamination. Subtraction of the excess carbon quantity then allows the calculation of a corrected elemental composition that can be compared to the expected stoichiometry (Table I). The results in Table I show that both N and O percentages are close to the expected stoichiometry of the sample.

Binding Energy Scale Calibration

The importance of a coherent and consistent approach to the binding energy (BE) scale calibration in XPS analysis has recently been highlighted.[24,25] As already mentioned, for organic compounds the adventitious carbon contribution to the C 1s emission is often used as an internal standard for the BE, although sometimes emission from another characteristic group containing carbon has been used.[25,26,33,34] Consistency in the accounting for the adventitious carbon contribution in the elemental analysis and in the fitting analysis of the C 1s emission line improves the accuracy and precision of the binding energy calibration. We generally find that this method ensures not only consistency of the binding energy scales between measurements taken on different spectrometers, but it also enables the

Table I. Element and adventitious carbon (C_{adv}) percentages compared to sample stoichiometries, including corrected values for N and O after removal of the C_{adv} contributions

	% C			% N			% O		
	Expected	Measured	C_{adv}	Expected	Measured	Corr.	Expected	Measured	Corr.
IN24DNBA	54.2	70.5	16.3	16.6	12.8	18.7	29.2	16.7	27.1
IN35DNBA	54.2	64.2	10	16.6	15.0	18.6	29.2	20.8	27.2
INPA	66.7	72.6	5.9	13.3	10.2	12.6	20.0	17.2	20.7
IN	66.7	70.8	4.1	22.2	18.2	20.9	11.1	11.0	12.4

use of absolute binding energies with accuracy on the order of ±0.1 eV to identify the chemical state of a sample. In the present study, we will determine absolute N 1s binding energies in this manner to characterise and classify hydrogen bonds and protonated moieties.[7–14,29]

Results

C 1s Emission and Binding Energy Scale Calibration

Table I summarises the results of the elemental analysis of pure isonicotinamide (IN) and the three IN complexes examined in this paper. As measured, excess carbon (C_{adv}) is evident in all data, indicating significant adventitious carbon contamination that ranges from 4.1% in IN to 16.3% in IN24DNBA. Adventitious carbon contamination is unavoidable and stems from the small concentrations of surface-active contaminants that are present even in the purest solvents and chemicals, alongside ubiquitous environmental contaminants introduced by handling materials in a biological environment; even after the most thorough cleaning, glass vessels used in the laboratory have remaining surface contamination on the order of a single molecular overlayer.[33–35] After subtracting the adventitious carbon percentage from the elemental analysis corrected values for the % contributions of N and O are obtained, which are in good agreement with the expected N and O stoichiometry of the materials (Table 1). C_{adv} also gives the fraction of C 1s signal that must be attributed to adventitious carbon. Locating this intensity in the C 1s emission line profile allows a precise calibration of the BE scale to 285.0 eV at the centre of the C_{adv} contribution. The expected functional group stoichiometry informs the relative intensities of the other C 1s component peaks, together with literature values for their BEs.[36] With these constraints in place, the C 1s fits presented in Figure 2 were obtained. The parameters of the components in these fits are summarised in Table II.

Table II. Best fit binding energies (eV), intensities (a.u.) and FWHMs (eV) for the fitted components to the C 1s emission

		O−C=O	N−C=O	−(C−X)=	−CH=/C_{adv}
IN24DNBA	BE / eV	288.9	288.1	286.3	285.0
	I / a.u.	89.2	89.2	249.3	304.1
	FWHM / eV	1.45	1.45	1.45	1.67
IN35DNBA	BE / eV	289.0	288.2	286.2	285.0
	I / a.u.	101.0	101.0	267.7	285.8
	FWHM / eV	1.56	1.56	1.56	1.64
INPA	BE / eV	289.1	288.4	286.2	285.0
	I / a.u.	133.6	133.6	259.8	412.8
	FWHM / eV	1.45	1.45	1.45	1.60
IN	BE / eV		287.9		285.0
	I / a.u.	n/a	126.5	n/a	373.9
	FWHM / eV		1.56		1.74

Given that IN and its three complexes do not contain any aliphatic hydrocarbon moieties (only aromatic groups), one would perhaps expect that the adventitious contamination intensity appears on the high BE shoulder to the aromatic emission peak (−CH=), which for unsubstituted aromatic carbons is often found at 0.2-0.3 eV lower BE than the emission from aliphatic hydrocarbons.[36] However, there is no significant evidence for a separate adventitious hydrocarbon line in the data, probably because it coincides with the emission from IN, in which the electronegative pyridinic nitrogen appears to increase the C 1s BE of the unsubstituted aromatic ring carbons somewhat. For the three salts, the nitro and carboxylic acid substituents in the co-formers appear to have a similar effect on the unsubstituted aromatic carbons. The unsubstituted aromatic hydrocarbon and adventitious carbon contributions were therefore fitted as a single line that was used as the internal BE reference at 285.0 eV (note other values are sometimes used for calibration, e.g. 284.8 eV).[29] We would like to emphasise that the fits summarised in Table II are in very good agreement both with the expected stoichiometry and the excess adventitious carbon signal indicated by the elemental analysis. We will show in the next section that this calibration of the BE results in N 1s BEs of 406.2 eV and 406.3 eV for the nitro groups in IN24DNBA and IN35DNBA, respectively (Figure 3), is in excellent agreement with all nitro N 1s BEs in our previous studies.[12,14] We are therefore confident that the presented C 1s analysis procedure represents best practice for a BE scale calibration based on the C 1s emission line.[24] This procedure was used in all our previous XPS studies of organic systems, which have produced a self-consistent set of binding energy values for various functional groups.[7–14]

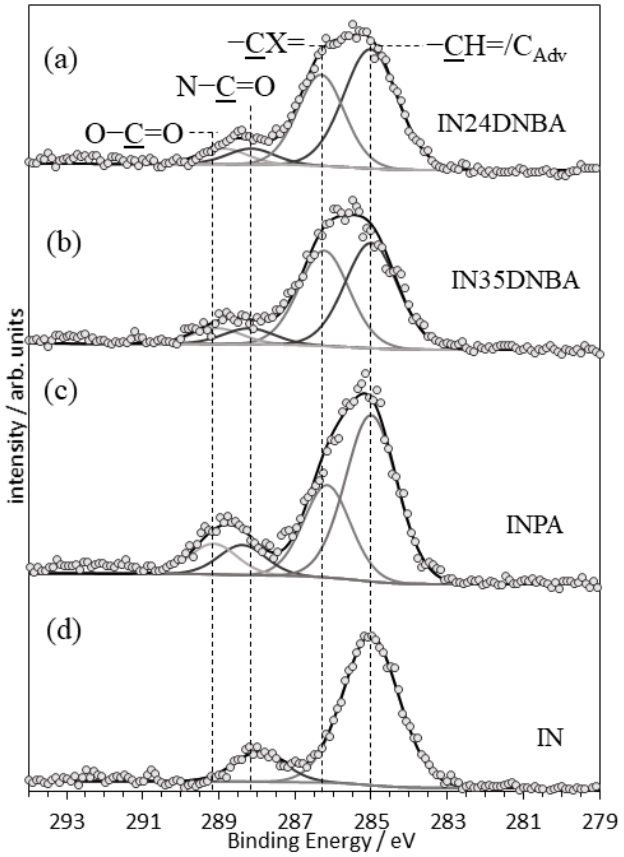

Figure 2. C 1s emission lines with best-fit components for the carboxylic acid (O−C=O) group, the amide (N−C=O) group from IN, aromatic carbons with electronegative substituents in DNBAs and PA (−(CX)=, with X = COOH, NO_2), unsubstituted aromatic carbons (−CH=), and adventitious carbon (C_{Adv}). (a) IN24DNBA, (b) IN35DNBA, (c) INPA and (d) pure isonicotinamide. The binding energy scale was calibrated at 285.0 eV with respect to the adventitious carbon contamination (Adv) emission, which is superimposed over the emission from the aromatic carbons (−C=).

N 1s Emission

As in our previous studies of organic salts and co-crystals, we use the BE of the N 1s emission line of the proton acceptor group to classify the donor-acceptor interaction.[7–9,11,12] Figure 3 shows the fits to the N 1s emission lines for the three IN complexes alongside that of pure IN, and Table III contains the parameters used for the fits. We already mentioned that the C 1s BE calibration places the nitro group N 1s of IN24DNBA and IN35DNBA at BEs of 406.2 eV and 406.3 eV, respectively. These values are in excellent agreement with our previous results for nitro groups, suggesting accuracy and reproducibility on the order of ±0.1 eV for our BE calibration method, even across different XPS instruments.[12,14,22] In addition, during earlier measurements of these samples, we experienced some issues with sample charging and possible radiation damage (data available in the supplementary

material, Figure S2 and Figure S3). Despite these issues, the same consistent fitting could be applied (with additional components) and the same binding energies determined.

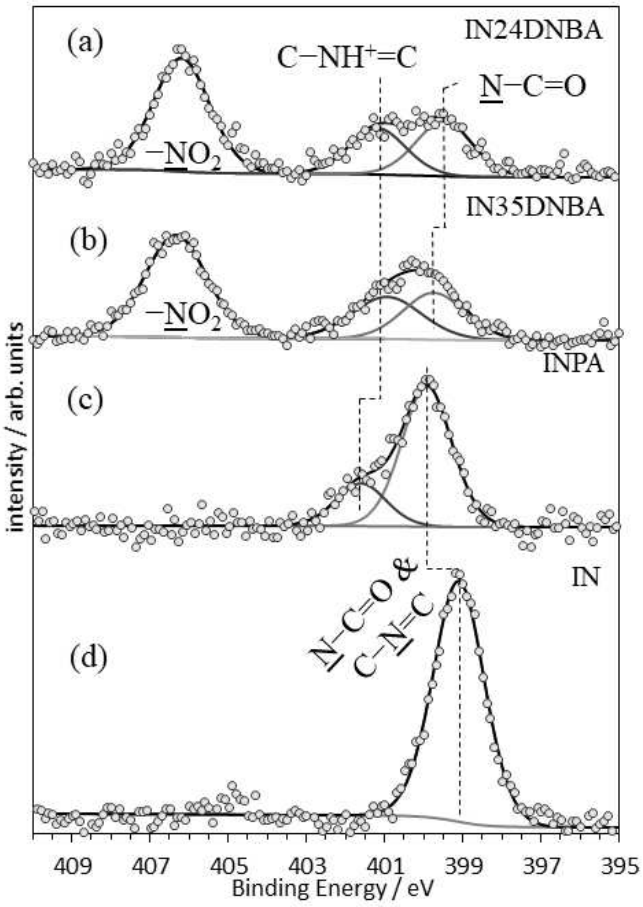

Figure 3. Nitrogen 1s XPS with fitted components for (a) IN24DNBA, (b) IN35DNBA, (c) INPA and (d) pure isonicotinamide. Binding energy scale calibration is taken with respect to the fitted adventitious carbon component peak.[29]

The BEs of observed N 1s components for the four materials are reported in Table III. Interestingly, although IN contains two chemically inequivalent nitrogen moieties (amide and pyridinic N) the BE of their N 1s emissions coincide within the spectral resolution achievable by experimental XPS, at the same BE of 399.1 eV. In line with this, the FWHM of the single emission line is, within the margins of error, identical to that of the individual N 1s components in the other N 1s spectra. The intensity of the combined emission line is consistent with the presence of two nitrogen atoms per formula unit (Table I), as expected from the stoichiometry of IN. Our experimental N 1s spectrum for IN agrees very well with a recently published spectrum,[15] but the assignment of the amide and pyridinic N 1s BEs differs markedly. In the recently published spectrum, two separate emission lines with very low

Table III. Best fit binding energies (eV), intensities (a.u.) and FWHMs (eV) for the fitted components to the N 1s emission. Single component fit describes both pyridinic and amide nitrogen indicated by *.

		N−C=O	C−N=C	C−NH⁺=C	−NO₂
IN24DNBA	BE / eV	399.5	n/a	401.2	406.2
	I / a.u.	636.7		617.9	813.8
	FWHM / eV	1.70		1.70	1.70
IN35DNBA	BE / eV	399.8	n/a	401.1	406.3
	I / a.u.	1078.4		1038.6	1309.1
	FWHM / eV	1.86		2.10	1.86
INPA	BE / eV	399.9*	399.9*	401.6	n/a
	I / a.u.	1093.1*	1093.1*	821.6	
	FWHM / eV	1.51*	1.51*	1.51	
IN	BE / eV	399.1*	399.1*	n/a	n/a
	I / a.u.	1184.9*	1184.9*		
	FWHM / eV	1.53*	1.53*		

FWHM were forced (through peak fitting constraints) to model the single combined N 1s emission line without justification, resulting in values of 398.6 eV for C−N=C and 400.6 eV for N−C=O (note we have added 0.2 eV to account for the use of 284.8 eV as the BE scale reference point in the previous paper).[15] Given that the FWHM of the overall N 1s emission is similar to that of the single N 1s components reported in that paper, the double-line fit is therefore difficult to justify, and we suggest adopting the value of 399.1 eV for the N 1s BE of both pyridinic and amide nitrogens.

For all three salts, the N 1s emission lines associated with IN in their crystal structures appear at higher BEs than for pure IN. For the amidic nitrogen (N−C=O), this is due to the interaction of the hydrogens with electronegative Brønsted acceptors in the crystal structure, resulting in withdrawal of electron density through N-H---O hydrogen bonds and a BE increase to 399.9 eV (INPA), 399.5 eV (IN24DNBA) and 399.8 eV (IN35DNBA). In the crystal structure of IN, a combination of N-H---O and weaker N-H---N hydrogen bonds are formed between amide groups, resulting in the lower BE. All three salts have a protonated pyridinic IN group (C−NH⁺=C), associated with N 1s BE shifts of 2.0 eV (IN35DNBA), 2.1 eV (IN24DNBA) and 2.5 eV (INPA) relative to pure IN, resulting in N 1s BEs of 401.1 eV, 401.2 eV and 401.6 eV, respectively. In INPA, half of the IN molecules have a hydrogen bond at the pyridinic nitrogen centre, characterised by a BE of 399.9 eV (C−N=C). All these results are fully consistent with previously observed BE ranges for hydrogen bonds in co-crystals (399

eV - 400 eV) and salts in which the nitrogen acceptor is protonated (401 eV – 402 eV).[7,8,11,12,14] Finally, we note that the intensities of all N 1s emission line components (Figure 3, Table III) agree very well with the stoichiometries expected from the crystal structures, indicating a consistent analysis.[28]

O 1s Emission

Due to the common presence of oxygen-containing contaminants on samples exposed to air (especially adsorbed H_2O and hydroxyl groups) the O 1s emission lines are usually harder to interpret than the N 1s emission lines. The O 1s emission lines are included here to indicate that a fully consistent interpretation across all emission spectra can be obtained, and to provide reference data for future studies of hydrogen bonding involving oxygen as donor and/or acceptor. Figure 4 and Table IV give the data with relevant fits and the parameters obtained, respectively.

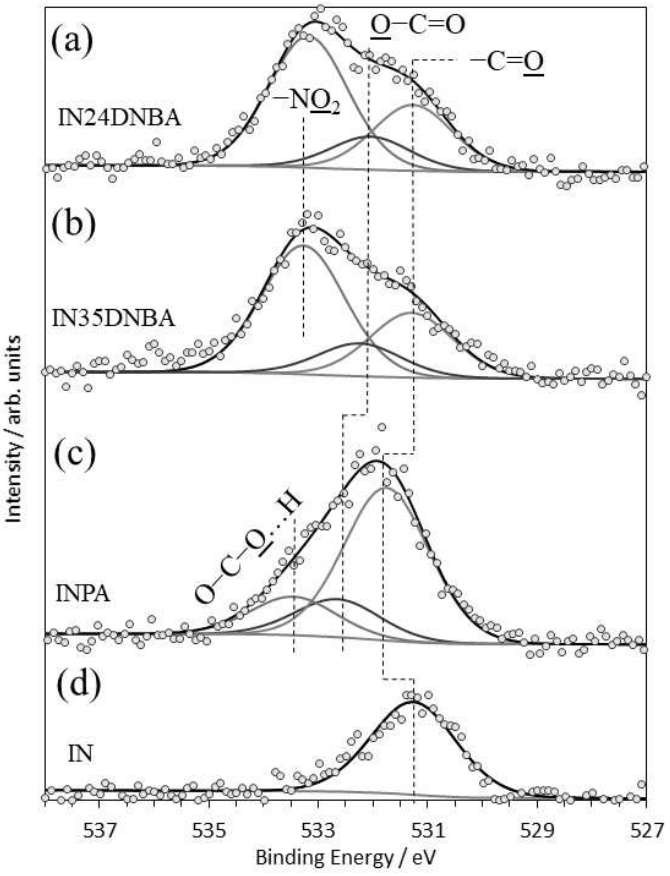

Figure 4. Oxygen 1s XPS with fitted components for (a) IN24DNBA, (b) IN35DNBA, (c) INPA and (d) pure isonicotinamide. Binding energy scale calibration is taken with respect to the fitted adventitious carbon peak.

Table IV. Best fit binding energies (eV), intensities (a.u.) and FWHMs (eV) for the fitted components to the O 1s emission

		−C=O	O−C=O	NO_2	O−C−O…H
IN24DNBA	BE / eV	531.3	532.1	533.2	
	I / a.u.	240.2	194.8	337.9	n/a
	FWHM / eV	1.71	1.71	1.71	
IN35DNBA	BE / eV	531.3	532.3	533.3	
	I / a.u.	241.1	197.3	337.5	n/a
	FWHM / eV	1.80	1.80	1.80	
INPA	BE / eV	531.8	532.7	n/a	533.5
	I / a.u.	389.3	229.4		233.3
	FWHM / eV	1.83	1.83		1.83
IN	BE / eV	531.3			
	I / a.u.	280.1	n/a	n/a	n/a
	FWHM / eV	1.93			

Discussion

The N 1s BEs determined by XPS show that we can distinguish protonation from hydrogen bonding and classify the examined materials correctly as salts, in line with previously reported BEs for other systems. The XPS classification agrees with the crystallographically determined hydrogen positions in the structures.[16]

The examined salts fall within the ΔpK_a range (0…3) that is associated with the salt-co-crystal-continuum, for which it is difficult to predict whether hydrogen bonding or proton transfer occurs.[37] In addition, for short donor-acceptor distances the associated potential wells may be separated by a low barrier, so that the hydrogen population in the crystal may reflect a dynamic equilibrium of occupancy across both potential wells.[10] *In extremis*, a continuum of positions between donor and acceptor is possible.[10] Even though the salts examined here exhibit such short donor-acceptor (N-O) distances (see Table S1), there is no evidence in the N 1s emission lines to suggest a disordered or continuum occupancy: there are no additional shoulders or broadening of the emission line components associated with proton transfer (see FWHMs in Table III). This is in line with the crystallographic analysis, which unequivocally identified proton transfer to the pyridinic nitrogen acceptor of IN. In the same study, the complexes were also investigated with a view to temperature dependent proton migration.[16] Allowing the proton to re-occupy the donor site requires a shallow potential energy surface, which is often observed in structures with short Brønsted donor-acceptor distances,[10,16]

However, the temperature-dependent analysis via Fourier difference electron density maps indicated only minor movement of the average hydrogen positions in the temperature range from 100 K to 350 K.[16] In fact, the analysis did not detect any significant proton migration for IN24DNBA and IN35DNBA.[16] For INPA, a slight shift of the average hydrogen positions towards the donor was detected, by about 0.05 Å.[16] This small shift is consistent with the pyridinic acceptor remaining protonated. This suggests that the potential well at the acceptors for all three salts is sufficiently deep to locate the proton, even at elevated temperatures. The weak temperature-dependent migration in INPA may be related to the local geometry of the donor-acceptor interaction: acceptor, hydrogen and donor positions are in a co-linear 180° arrangement. In contrast, they are arranged at an angle close to 160° in the DNBA complexes, which places the proton off the axis between donor and acceptor group.[16]

Table V. ΔpK_a values compared with N-H, N-O bond distances (from XRD)[12,16,37,38] and N 1s Binding Energy

	ΔpK_a	*D (N-H)*	*D (N-O)*	*N 1s BE*
IN24DNBA	2.18	1.05	2.60	401.2
IN35DNBA	0.94	1.08	2.54	401.1
INPA (salt)	0.72	1.10	2.55	401.6
INPA (co-crystal)	-1.90	1.66	2.70	399.9

Due to the short distance between donor and acceptor, the electron density at the donor site may be expected to influence the electrostatic potential at the acceptor group, and hence its N 1s binding energy. Indeed, this appears to be borne out by the low N 1s BEs (401.1 eV / 401.2 eV) for the protonated pyridinic nitrogen in IN24DNBA and IN35DNBA (Figure 5). These BEs represent the lowest values we have observed so far for any organic salt system (Figure 5). Therefore, while the barrier to the donor potential appears to be high enough to prevent, at least up to 350 K, significant re-occupation of the donor position, the proximity of the donor potential appears to reduce the depth of the potential well at the acceptor. This effect may be enhanced by the off-axis position of the proton. For INPA, the N 1s BE of the protonated pyridinic is higher (Figure 5), again in line with a potential well that is sufficiently deep to localize the transferred proton, but in this case with less influence of the electrostatic donor potential. The latter may be due to shielding of the donor potential by the

electrostatic field of the co-linearly aligned proton. These considerations highlight the importance of the local geometry for classifying Brønsted interactions.

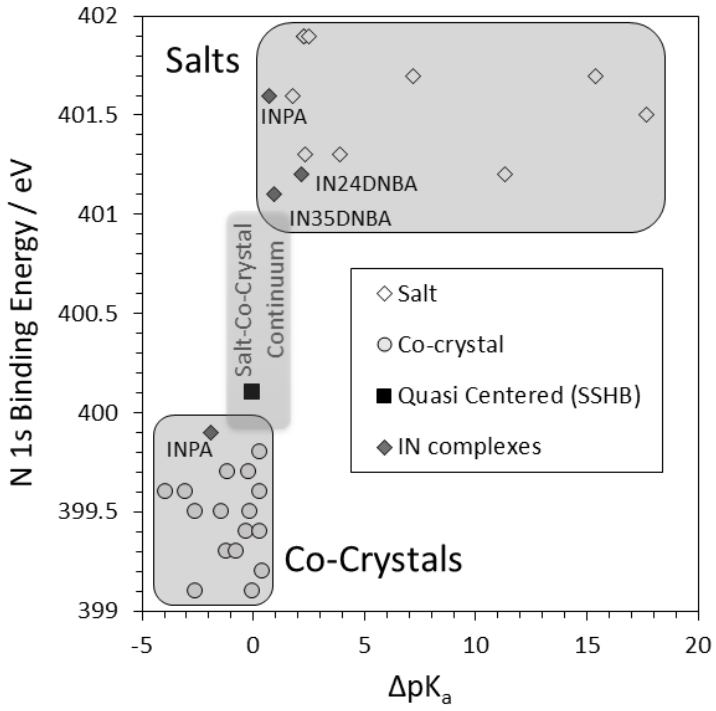

Figure 5. Relationship between the N 1s core level binding energies (XPS) with the ΔpK_a for a range of salt, co-crystal and short strong hydrogen bonded crystal structures, including the three complexes investigated here.[12]

It is interesting to examine the salt N 1s BEs in comparison with previously studied salt and co-crystal systems. First, we examine the BEs as a function of ΔpK_a (Figure 5), i.e., the difference between the acid dissociation constant (pK_a) of acid and base [$\Delta pK_a = pK_a$ (base) – pK_a (acid)], known as the pK_a slide rule.[3] This empirical set of rules is generally defined such that a value of $\Delta pK_a > 3$ means a salt is formed, $\Delta pK_a < 0$ means a co-crystal is formed and $0 < \Delta pK_a < 3$ is not definitive.[3] Using the standard pK_a values for the components, the ΔpK_a values for the three complexes are shown in Table V.[19,38,39] The standard hydrogen bond between phthalic acid and half of the IN molecules in INPA is associated with a ΔpK_a of –1.90, so the empirical relationship correctly predicts the absence of proton transfer.[3,37] The three ΔpK_a values associated with proton transfer fall within the salt-co-crystal continuum range, where the empirical relationship is not sufficient to determine whether or not proton transfer occurs.[3] Figure 5 shows the relationship between the N 1s BE and the ΔpK_a value against a range of structures from the literature.[12] It is evident that the two clusters of N 1s BEs reliably classify systems into salt and co-crystals, including in the salt-co-crystal continuum range, $0 < \Delta pK_a < 3$. However, with the data from this paper included, there is a region of overlap around $\Delta pK_a = 0 \ldots 1$, which we have not observed

previously to the same extent.[12] These consolidated XPS results thus confirm that ΔpK_a in this range is not sufficient to predict which interaction will occur, whilst the binding energy provides a fully consistent approach to distinguishing between the two distinct interactions.

We note, however, that there is a clear separation of salt and co-crystal BEs when the XPS N 1s BE results are plotted as a function of the distance between nitrogen acceptor and proton, d(N-H). While this distance and the binding energy are impacted by many factors, including the surrounding electronic environment, donor-acceptor distance and the interaction angle, it provides an insight into the effect of the proton acceptor distance on the core electronic binding energy. It appears that protonation is associated with distances below 1.15 Å, whereas the shortest distance in a hydrogen bond is about 1.38 Å. Systems in the salt-co-crystal continuum would then appear to be associated with intermediate distances. So far, only one previously studied system can be confidently placed in this range,[10] and more systems should be evaluated to create a better understanding in this range of the diagram.

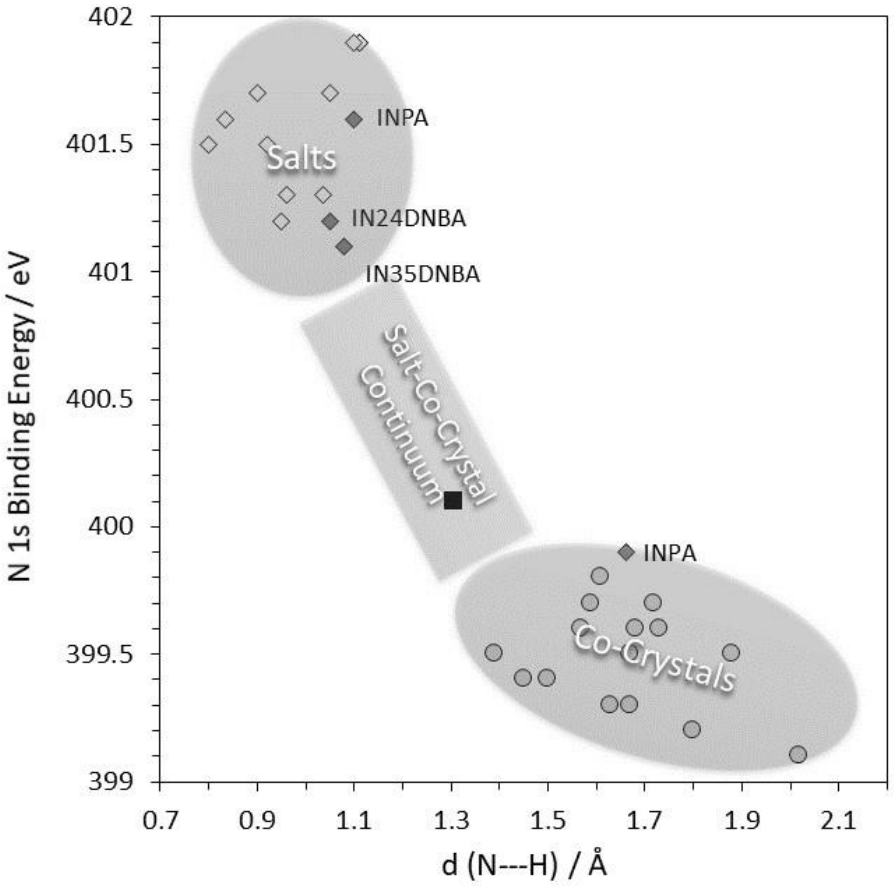

Figure 6. Relationship between the N 1s core level binding energies (XPS) with the distance between the Brønsted proton and the acceptor nitrogen in a range of crystal structures including the three complexes investigated here. All distances determined using X-ray diffraction and sourced from the Cambridge Structural Database.[40]

This classification is fully consistent with the physical process, whereby proton transfer leads to a shorter proton acceptor distance. The most important aspect of Figure 6 is the consistency with which salts and co-crystals are separated uniquely by the electron binding energy, with co-crystals between 399 eV – 400 eV, and salts between 401 eV – 402 eV.[7,12,14,30] This is the case despite the measurements being from a range of independent investigations carried out by our group over the last decade. Using the analysis procedure laid out in the present paper is key for achieving this consistency. Therefore, we suggest that the effect on the binding energy from the donor acceptor distance and interaction angle is sufficiently small such that the binding energy will always lie within the range we have consistently observed, with the variation within that range due to additional effects, including proton-acceptor distance, donor-acceptor distance as well as the angle between acceptor, proton and donor.

Conclusions

N 1s BEs determined by XPS correctly classified the nature of Brønsted interactions in three two-component isonicotinamide systems with short donor-acceptor distances. We demonstrated the data analysis procedure allowing full quantification of all data in a comprehensive XPS data set, including the quantitative fitting analysis of all (C, N, O) emission lines, the identification of the carbon contamination signal and the calibration of the binding energy scale through the C 1s emission line. For all three compounds, INPA, IN24DNBA and IN35DNBA, the N 1s BEs indicated the protonation of the pyridinic nitrogen of the isonicotinamide component. The results for IN24DNBA and IN35DNBA indicate that the transferred proton experiences significant electrostatic attraction from the donor group, resulting in low BEs that place these systems on the edge of the salt-co-crystal continuum. The transferred proton in INPA is aligned co-linearly with the donor and the acceptor and appears to shield the acceptor from the influence of the electron density at the donor. Summarising all XPS results we have obtained for other salt and co-crystal systems as a function of ΔpK_a values highlights the predictive failure of the ΔpK_a method in the ΔpK_a region from 0 to about 1. In this region, there appears to be higher predictive power in the distance between the acceptor group and the proton, suggesting a universal dependence of the observed N 1s binding energy on the distance to the proton.

Acknowledgements

XPS data were collected at the Versatile X-ray Spectroscopy Facility (VXSF), which is based in the Bragg Centre at the University of Leeds and funded by the Sir Henry Royce Institute (EPSRC Grants EP/R00661X/1, EP/S019367/1 and EP/P022464/1). PTE gratefully acknowledges a PhD studentship funded jointly by Diamond and through the EPSRC Doctoral Training Partnership (DTP) with the University of Leeds (EPSRC Grant EP/R513258/1). SLMS thanks the Royal Academy of Engineering, Diamond Light Source Ltd and Infineum UK for support of the Bragg Centenary Chair, and for financial support from the Future Continuous Manufacturing and Advanced Crystallisation (CMAC) Hub (EPSRC Grant EP/P006965/1). All data supporting this study are provided either in the results section of this paper or in the ESI accompanying it.

Supporting Information: Survey spectra of all samples, hydrogen bonding parameters and spectra showing the effects of radiation damage and sample charging.

References

(1) Blagden, N.; de Matas, M.; Gavan, P. T.; York, P. Crystal Engineering of Active Pharmaceutical Ingredients to Improve Solubility and Dissolution Rates. *Advanced Drug Delivery Reviews*. July 30, **2007**, 617–630. DOI: 10.1016/j.addr.2007.05.011.

(2) Etter, M. C. Encoding and Decoding Hydrogen-Bond Patterns of Organic Compounds. *Accounts of Chemical Research* **1990**, *23* (4), 120–126.

(3) Gilli, P.; Pretto, L.; Bertolasi, V.; Gilli, G. Predicting Hydrogen-Bond Strengths from Acid-Base Molecular Properties. The pK(a) Slide Rule: Toward the Solution of a Long-Lasting Problem. *Accounts of Chemical Research* **2009**, *42* (1), 33–44. DOI: 10.1021/ar800001k.

(4) Aakeröy, C. B.; Fasulo, M. E.; Desper, J. Cocrystal or Salt: Does It Really Matter? *Molecular Pharmaceutics* **2007**, *4* (3), 317–322. DOI: 10.1021/mp060126o.

(5) Childs, S. L.; Stahly, G. P.; Park, A. The Salt-Cocrystal Continuum: The Influence of Crystal Structure on Ionization State. *Molecular Pharmaceutics* **2007**, *4* (3), 323–338. DOI: 10.1021/mp0601345.

(6) Wouters, J.; Quéré, L. *Pharmaceutical Salts and Co-Crystals*; Drug Discovery; The Royal Society of Chemistry, **2012**. DOI: 10.1039/9781849733502.

(7) Stevens, J. S.; Byard, S. J.; Schroeder, S. L. M. Salt or Co-Crystal? Determination of Protonation State by X-Ray Photoelectron Spectroscopy (XPS). *Journal of Pharmaceutical Sciences* **2010**, *99* (11), 4453–4457. DOI: 10.1002/jps.22164.

(8) Stevens, J. S.; Byard, S. J.; Schroeder, S. L. M. Characterization of Proton Transfer in Co-Crystals by X-Ray Photoelectron Spectroscopy (XPS). *Crystal Growth & Design* **2010**, *10* (3), 1435–1442. DOI: 10.1021/cg901481q.

(9) Stevens, J. S.; Byard, S. J.; Muryn, C. A.; Schroeder, S. L. Identification of Protonation State by XPS, Solid-State NMR, and DFT: Characterization of the Nature of a New Theophylline Complex by Experimental and Computational Methods. *J Phys Chem B* **2010**, *114* (44), 13961–13969. DOI: 10.1021/jp106465u.

(10) Stevens, J. S.; Coultas, S.; Jaye, C.; Fischer, D. A.; Schroeder, S. L. M. Core Level Spectroscopies Locate Hydrogen in the Proton Transfer Pathway-Identifying Quasi-Symmetrical Hydrogen Bonds in the Solid State. *Physical Chemistry Chemical Physics* **2020**, *22* (9), 4916–4923. DOI: 10.1039/c9cp05677g.

(11) Stevens, J. S.; Newton, L. K.; Jaye, C.; Muryn, C. A.; Fischer, D. A.; Schroeder, S. L. M. Proton Transfer, Hydrogen Bonding, and Disorder: Nitrogen Near-Edge X-Ray Absorption Fine Structure and X-Ray Photoelectron Spectroscopy of Bipyridine-Acid Salts and Co-Crystals. *Crystal Growth & Design* **2015**, *15* (4), 1776–1783. DOI: 10.1021/cg5018278.

(12) Stevens, J. S.; Byard, S. J.; Seaton, C. C.; Sadiq, G.; Davey, R. J.; Schroeder, S. L. M. Proton Transfer and Hydrogen Bonding in the Organic Solid State: A Combined XRD/XPS/SsNMR Study of 17 Organic Acid-Base Complexes. *Physical Chemistry Chemical Physics* **2014**, *16* (3), 1150–1160. DOI: 10.1039/c3cp53907e.

(13) Wang, T.; Stevens, J. S.; Vetter, T.; Whitehead, G. F. S.; Vitorica-Yrezabal, I. J.; Hao, H. X.; Cruz-Cabeza, A. J. Salts, Cocrystals, and Ionic Cocrystals of a "Simple" Tautomeric Compound. *Crystal Growth & Design* **2018**, *18* (11), 6973–6983. DOI: 10.1021/acs.cgd.8b01159.

(14) Stevens, J. S.; Byard, S. J.; Seaton, C. C.; Sadiq, G.; Davey, R. J.; Schroeder, S. L. M. Crystallography Aided by Atomic Core-Level Binding Energies: Proton Transfer versus Hydrogen Bonding in Organic Crystal Structures. *Angewandte Chemie-International Edition* **2011**, *50* (42), 9916–9918. DOI: 10.1002/anie.201103981.

(15) Tothadi, S.; Shaikh, T. R.; Gupta, S.; Dandela, R.; Vinod, C. P.; Nangia, A. K. Can We Identify the Salt-Cocrystal Continuum State Using XPS? *Crystal Growth and Design* **2021**, *21* (2), 735–747. DOI: 10.1021/acs.cgd.0c00661.

(16) Saunders, L. K.; Nowell, H.; Hatcher, L. E.; Shepherd, H. J.; Teat, S. J.; Allan, D. R.; Raithby, P. R.; Wilson, C. C. Exploring Short Strong Hydrogen Bonds Engineered in Organic Acid Molecular Crystals for Temperature Dependent Proton Migration Behaviour Using Single Crystal Synchrotron X-Ray Diffraction (SCSXRD). *CrystEngComm* **2019**, *21* (35), 5249–5260. DOI: 10.1039/C9CE00925F.

(17) Saunders, L. K.; Nowell, H.; Spencer, H. C. E.; Hatcher, L. E.; Shepherd, H. J.; Thomas, L. H.; Jones, C. L.; Teat, S. J.; Raithby, P. R.; Wilson, C. C. Tuning Charge-Assisted and Weak Hydrogen Bonds in Molecular Complexes of the Proton Sponge DMAN by Acid Co-Former Substitution. *Crystengcomm* **2018**, *20* (22), 3074–3083. DOI: 10.1039/c8ce00443a.

(18) Schmidtmann, M.; Gutmann, M. J.; Middlemiss, D. S.; Wilson, C. C. Towards Proton Transfer in Hydrogen Bonded Molecular Complexes: Joint Experimental and Theoretical Modelling and an Energy Scale for Polymorphism. *Crystengcomm* **2007**, *9* (9), 743–745. DOI: 10.1039/b709136m.

(19) Sánchez-Férez, F.; Ejarque, D.; Calvet, T.; Font-Bardia, M.; Pons, J. Isonicotinamide-Based Compounds: From Cocrystal to Polymer. *Molecules* **2019**, *24* (22). DOI: 10.3390/molecules24224169.

(20) Saunders, L. K.; Pallipurath, A. R.; Gutmann, M. J.; Nowell, H.; Zhang, N.; Allan, D. R. A Quantum Crystallographic Approach to Short Hydrogen Bonds. *CrystEngComm* **2021**. DOI: 10.1039/d1ce00355k.

(21) Steiner, T.; Majerz, I.; Wilson, C. C. First O-H-N Hydrogen Fond with a Centered Proton Obtained by Thermally Induced Proton Migration. *Angewandte Chemie-International Edition* **2001**, *40* (14), 2651–2654 DOI: 10.1002/1521-3773(20010716)40:14<2651::aid-anie2651>3.0.co;2-2.
(22) Deshkovskaya, A.; Shchukarev, A. XPS Study of Fluorine Implantation Unduced Centres in Fused Silica; *10th International Conference "Interaction of Radiation with Solids"* 2013.
(23) Stevens, J. S.; Gainar, A.; Jaye, C.; Fischer, D. A.; Schroeder, S. L. M.; Iop. NEXAFS and XPS of P-Aminobenzoic Acid Polymorphs: The Influence of Local Environment. In *16th International Conference on X-ray Absorption Fine Structure (XAFS)*; Journal of Physics Conference Series; **2016**; Vol. 712 DOI: 10.1088/1742-6596/712/1/012133.
(24) Greczynski, G.; Hultman, L. Compromising Science by Ignorant Instrument Calibration—Need to Revisit Half a Century of Published XPS Data. *Angewandte Chemie* **2020**, *132* (13), 5034–5038. DOI: 10.1002/ange.201916000.
(25) Greczynski, G.; Hultman, L. X-Ray Photoelectron Spectroscopy: Towards Reliable Binding Energy Referencing. *Progress in Materials Science*. Elsevier Ltd January 1, 2020. DOI: 10.1016/j.pmatsci.2019.100591.
(26) Baer, D. R.; Artyushkova, K.; Cohen, H.; Easton, C. D.; Engelhard, M.; Gengenbach, T. R.; Greczynski, G.; Mack, P.; Morgan, D. J.; Roberts, A. XPS Guide: Charge Neutralization and Binding Energy Referencing for Insulating Samples. *Journal of Vacuum Science & Technology A* **2020**, *38* (3), 031204. DOI: 10.1116/6.0000057.
(27) Dietrich, P. M.; Bahr, S.; Yamamoto, T.; Meyer, M.; Thissen, A. Chemical Surface Analysis on Materials and Devices under Functional Conditions – Environmental Photoelectron Spectroscopy as Non-Destructive Tool for Routine Characterization. *Journal of Electron Spectroscopy and Related Phenomena* **2019**, *231*, 118–126. DOI: 10.1016/j.elspec.2017.12.007.
(28) Fairley, N.; Carrick, A. *The Casa Cookbook: Recipes for XPS Data Processing*; Casa cookbook; Acolyte Science: Knutsford, Cheshire, 2005.
(29) Shard, A. G. Practical Guides for X-Ray Photoelectron Spectroscopy: Quantitative XPS. *Journal of Vacuum Science & Technology A* **2020**, *38* (4), 041201. DOI: 10.1116/1.5141395.
(30) Stevens, J. S.; Schroeder, S. L. M. Quantitative Analysis of Saccharides by X-Ray Photoelectron Spectroscopy. *Surface and Interface Analysis* **2009**, *41* (6), 453–462. DOI: 10.1002/sia.3047.
(31) Reed, B. P.; Cant, D. J. H.; Spencer, S. J.; Carmona-Carmona, A. J.; Bushell, A.; Herrera-Gómez, A.; Kurokawa, A.; Thissen, A.; Thomas, A. G.; Britton, A. J.; Bernasik, A.; Fuchs, A.; Baddorf, A. P.; Bock, B.; Theilacker, B.; Cheng, B.; Castner, D. G.; Morgan, D. J.; Valley, D.; Willneff, E. A.; Smith, E. F.; Nolot, E.; Xie, F.; Zorn, G.; Smith, G. C.; Yasufuku, H.; Fenton, J. L.; Chen, J.; Counsell, J. D. P.; Radnik, J.; Gaskell, K. J.; Artyushkova, K.; Yang, L.; Zhang, L.; Eguchi, M.; Walker, M.; Hajdyła, M.; Marzec, M. M.; Linford, M. R.; Kubota, N.; Cortazar-Martínez, O.; Dietrich, P.; Satoh, R.; Schroeder, S. L. M.; Avval, T. G.; Nagatomi, T.; Fernandez, V.; Lake, W.; Azuma, Y.; Yoshikawa, Y.; Shard, A. G. Versailles Project on Advanced Materials and Standards Interlaboratory Study on Intensity Calibration for X-Ray Photoelectron Spectroscopy Instruments Using Low-Density Polyethylene. *Journal of Vacuum Science & Technology A* **2020**, *38* (6), 063208. DOI: 10.1116/6.0000577.
(32) Zommer, L. Determination of the Spectrometer Transmission Function for XPS Quantitative Analysis. *Vacuum* **1995**, *46* (5–6), 617–620. DOI: 10.1016/0042-207X(94)00143-X.

(33) ISO 15472:2010. Surface Chemical Analysis X-Ray Photoelectron Spectrometers Calibration of Energy Scales. ISO: Geneva 2010.
(34) ASTM E1523-15. Standard Guide to Charge Control and Charge Referencing Techniques in X-Ray Photoelectron Spectroscopy (ASTM International, West Conshohocken, PA, 2015)
(35) Mangolini, F.; McClimon, J. B.; Rose, F.; Carpick, R. W. Accounting for Nanometer-Thick Adventitious Carbon Contamination in X-Ray Absorption Spectra of Carbon-Based Materials. *Analytical Chemistry* **2014**, *86* (24), 12258–12265. DOI: 10.1021/ac503409c.
(36) Naumkin, A. v.; Kraut-Vass, A.; Gaarenstroom, S. W.; Powell, C. J. NIST X-ray Photoelectron Spectroscopy Reference Database 20 Version 4.1, DOI: 10.18434/T4T88K
(37) Chen, J. G.; McAllister, M. A.; Lee, J. K.; Houk, K. N. Short, Strong Hydrogen Bonds in the Gas Phase and in Solution: Theoretical Exploration of PKa Matching and Environmental Effects on the Strengths of Hydrogen Bonds and Their Potential Roles in Enzymatic Catalysis. *Journal of Organic Chemistry* **1998**, *63* (14), 4611–4619. DOI: 10.1021/jo972262y.
(38) Williams R. *PKa Data Compiled by R. Williams,* 2011 https://organicchemistrydata.org/hansreich/resources/pka/pka_data/pka-compilationwilliams.pdf [Online accessed on 20/01/2021].
(39) Harding, A. P. The Prediction of Mutagenicity and pKa for Pharmaceutically Relevant Compounds Using “Quantum Chemical Topology” Descriptors; PhD Thesis, The University of Manchester, 2010.
(40) Groom, C. R.; Bruno, I. J.; Lightfoot, M. P.; Ward, S. C. The Cambridge Structural Database. *Acta Crystallographica Section B: Structural Science, Crystal Engineering and Materials* **2016**, *72* (2), 171–179. DOI: 10.1107/S2052520616003954.

For Table of Contents use only

Proton Transfer on the Edge of the Salt/Co-Crystal Continuum: X-ray Photoelectron Spectroscopy (XPS) of Three Isonicotinamide Salts

Paul T. Edwards, Lucy K. Saunders, Anuradha R. Pallipurath, Andrew J. Britton, Elizabeth A. Willneff, Elizabeth J. Shotton, Sven L. M. Schroeder

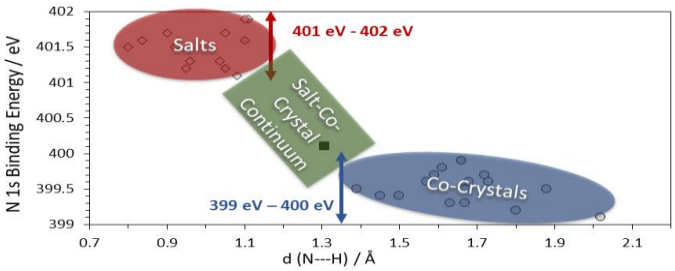

We show how careful calibration of the binding energy scale allows X-ray photoelectron spectroscopy to be used to consistently determine the nature of Brønsted proton donor-acceptor interactions in the region at the edge of the salt-cocrystal continuum through a binding energy shift of +2 eV between co-crystal and salt structures.